Journal of Statistical Physics, Vol. 107, Nos. 1/2, April 2002 (© 2002)

Entropy Function Approach to the Lattice Boltzmann Method

Santosh Ansumali[1] and Iliya V. Karlin[1]

Received February 26, 2001; accepted June 25, 2001

In this paper, we present the construction of the Lattice Boltzmann method equipped with the H-theorem. Based on entropy functions whose local equilibria are suitable to recover the Navier–Stokes equations in the framework of the Lattice Boltzmann method, we derive a collision integral which enables simple identification of transport coefficients, and which circumvents construction of the equilibrium. We discuss performance of this approach as compared to the standard realizations.

KEY WORDS: Kinetic theory; H-theorem; Lattice Boltzmann method; stability.

1. INTRODUCTION

The Lattice Boltzmann method (hereafter LBM) for simulations of complex hydrodynamic phenomena has received much attention over the past decade.[1] In the LBM, macroscopic equations are not addressed directly by a conventional discretization procedure, rather fully discrete kinetic models are constructed in such a way that (i) their long time, large scale limit matches the macroscopic dynamics in question, and (ii) they allow a relatively simple numerical implementation. In its present and mostly used form, the LBM is based on (i) a polynomial ansatz with tailored properties for the local equilibrium, and (ii) a single relaxation time model (hereafter SRTM) for the relaxation (collision) term. The SRTM has been borrowed from the well known Bhatnagar–Gross–Krook approximation of the Boltzmann collision integral of the classical kinetic theory. The resulting method is known as the LBGK model.[2, 3] However,

[1] ETH Zürich, Department of Materials, Institute of Polymers, ETH-Zentrum, ML J 19, Sonneggstr. 3, CH-8092 Zürich, Switzerland; e-mail: ansumali@ifp.mat.ethz.ch and ikarlin@ifp.mat.ethz.ch

0022-4715/02/0400-0291/0 © 2002 Plenum Publishing Corporation

in spite of impressive evidences of successful applications of the present realization of LBM,[1] theoretical development of the method is far from being over. One of the problems, recognized by many authors, is the problem of numerical stability.[1, 4, 5] For example, in the framework of the LBM starting with the work[6] many simulations of high Reynolds number flows has been successfully performed (see, for detail, refs. 1 and 7). However, progress on stability may be needed to go beyond existing state of the arts like spectral methods in simple geometries.

It has been discussed for some time in the literature[1, 4, 5, 8, 9] that stability of the LBM could be improved if the method could be based on an analog of the Boltzmann H-theorem. The goal of this work is to summarize progress made in this direction in recent years.[4, 5, 8, 9] First, we will present entropy functions which reproduces the correct hydrodynamics within the accuracy of the Lattice Boltzmann method for a particular choice of the Lattice. Next, based on the knowledge of these entropy functions, we develop a realization of the Lattice Boltzmann method with the H-theorem built in. We will discuss how using these entropy functions a SRTM collision integral, which circumvents need of a polynomial ansatz for the local equilibrium, can be constructed. Finally, some numerical tests will be presented to show unconditional stability of this new class of the Lattice Boltzmann models (ELBM hereafter).[5, 8, 9]

2. OVERVIEW OF THE LBM

In the Lattice Boltzmann method,[1] one considers populations of fictitious particles $\mathbf{f}$ with ith component as $f_i(\mathbf{r}, t)$, where $i = 1,\ldots, b$ labels discrete velocities $\mathbf{c}_i$. The set of discrete velocities, which can also include a zero vector ("rest population"), is associated with outgoing links at each site $\mathbf{r}$ of a regular isotropic lattice. Populations are updated at discrete time steps t according to an equation,

$$f_i(\mathbf{r}+\mathbf{c}_i, t+1)-f_i(\mathbf{r}, t) = \Delta_i \tag{1}$$

In the following, we shall restrict our attention to the isothermal Navier–Stokes equation. For this case, the collision integral $\mathbf{\Delta}$ must obey only the local conservation laws,

$$\langle\{\mathbf{1}, \mathbf{c}_\alpha\} \,|\, \mathbf{\Delta}\rangle = \{0, 0\} \tag{2}$$

where, we denote scalar product of b-dimensional vectors $\mathbf{x}$ and $\mathbf{y}$ as $\langle \mathbf{x} \,|\, \mathbf{y}\rangle = \sum_{i=1}^{b} x_i y_i$, the Cartesian components of d-dimensional vector as

$\alpha = 1,\ldots, d$, and $(1,\ldots, 1)$ as **1**. Local hydrodynamic quantities (the mass density and the momentum density respectively) are defined as,

$$\langle \{\mathbf{1}, \mathbf{c}_\alpha\} \mid \mathbf{f} \rangle = \{\rho, \rho u_\alpha\} \tag{3}$$

If the long-time large-scale limit of Eq. (1) recovers the Navier–Stokes equation, then hydrodynamics is implemented in a fairly simple, fully discrete kinetic picture. To do so, the most popular choice is Bhatnagar–Gross–Krook approximation (hereafter BGK) for the collision integral and a polynomial ansatz for the equilibrium distribution. With the BGK approximation, the LBE equation (1) is given as

$$f_i(\mathbf{r}+\mathbf{c}_i, t+1) - f_i(\mathbf{r}, t) = -\frac{1}{2\tau}\left(f_i(\mathbf{r}, t) - f_i^{\mathrm{eq}}(\mathbf{r}, t)\right) \tag{4}$$

The equilibrium distribution ($\mathbf{f}^{\mathrm{eq}}$) are subjected to constraints fixed by the hydrodynamic fields,

$$\langle \{\mathbf{1}, \mathbf{c}_\alpha\} \mid \mathbf{f}^{\mathrm{eq}} \rangle = \{\rho, \rho u_\alpha\} \tag{5}$$

In addition, in order to recover the Navier–Stokes equation up to second-order accuracy in u, the local equilibrium must respect the condition for the stress tensor,

$$\sum_{i=1}^{b} c_{i\alpha} c_{i\beta} f_i^{\mathrm{eq}} = \rho u_\alpha u_\beta + \rho c_{\mathrm{s}}^2 \delta_{\alpha\beta} \tag{6}$$

where c_{s} is the speed of sound. Then a quadratic form of distribution function which satisfy these restriction is used.

3. ENTROPY FUNCTIONS FOR THE LBM

If the local equilibrium is supported by some entropy function, then the Lattice Boltzmann method can be equipped with the H-theorem,[10, 11] and stability problem can be studied in a controlled way. However, any approach which attempts to enhance stability via an H-theorem, must be able to recover the Navier–Stokes equations and the H-function must be found by lattice-dependent considerations.[4] For the case of one-dimensional three velocity and two-dimensional nine velocity lattice such entropy functions are known[4] and are given here for the sake of the completeness.

In the case of the one-dimensional lattice with spacing c, the velocity set at each lattice site consists of three velocities, $c_+ = c$, $c_- = -c$, and $c_0 = 0$. For this case entropy function is given as,[4]

$$H = f_0 \ln\left(\frac{f_0}{4}\right) + f_- \ln(f_-) + f_+ \ln(f_+) \tag{7}$$

In this particular case, it is actually possible to get analytically the equilibrium distribution.

$$\begin{aligned} f_0^{\mathrm{eq}} &= \frac{2\rho}{3}\left[2 - \sqrt{1+M^2}\right] \\ f_+^{\mathrm{eq}} &= \frac{\rho}{3}\left[\frac{uc - c_s^2}{2c_s^2} + \sqrt{1+M^2}\right] \\ f_-^{\mathrm{eq}} &= \frac{\rho}{3}\left[-\frac{uc + c_s^2}{2c_s^2} + \sqrt{1+M^2}\right] \end{aligned} \tag{8}$$

where, the $c_s^2 = c^2/3$ is the square of the sound velocity and $M^2 = u^2/c_s^2$ is the Mach number squared. However, result (8) is the exclusive case which does not happen in higher dimensions.

In a two-dimensional Cartesian coordinates system, for nine-velocity lattice ($2d9v$) the entropy function is given as,[4]

$$H = f_0 \ln\left(\frac{f_0}{8}\right) + \sum_{l=1}^{4} f_l \ln\left(\frac{f_l}{2}\right) + \sum_{l=5}^{8} f_l \ln(2f_l) \tag{9}$$

where, the discrete velocity vector set $\mathbf{c} = \{\mathbf{c}_x, \mathbf{c}_y\}$ is given as,

$$\mathbf{c}_x = (0, \quad 1, \quad 0, \quad -1, \quad 0, \quad 1, \quad -1, \quad -1, \quad 1)^T \tag{10}$$

$$\mathbf{c}_y = (0, \quad 0, \quad 1, \quad 0, \quad -1, \quad 1, \quad 1, \quad -1, \quad -1)^T \tag{11}$$

Local equilibria of these entropy functions satisfy the Eq. (6) up to the order of M^4.

4. LBM BASED ON THE ENTROPY FUNCTION

Knowledge of the perfect entropy function suggests realizations of the Lattice Boltzmann method which do not require an explicit expression for the local equilibrium. In the subsequent section, we formulate one of such realizations. Before doing this, however, we describe a general procedure which equips any realization with the H-theorem. Let us assume that the

collision integral $\mathbf{\Delta}(\mathbf{f})$ in the kinetic equation (1) is realized in such a way that it satisfies two conditions: (i) the conservation laws Eq. (2) (ii) the entropy production inequality, $\langle \nabla H \mid \mathbf{\Delta} \rangle \leqslant 0$, where ∇H is the gradient of the entropy function, while the equality sign implies $\mathbf{f} = \mathbf{f}^{eq}$. A collision integral which meets these requirements will be termed admissible. For instance, the standard BGK collision integral is admissible. For each pair of vectors $\{\mathbf{f}, \mathbf{\Delta}\}$ such that $f_i \geqslant 0$, we introduce an auxiliary population vector $\mathbf{f}^* = \mathbf{f} + \alpha^* \mathbf{\Delta}$. The scalar parameter α^* is derived as follows: Let us consider the equation

$$H(\mathbf{f}) = H(\mathbf{f} + \alpha \mathbf{\Delta}) \tag{12}$$

There are two cases classified by the number of solutions the Eq. (12) may have. In the first case, Eq. (12) has two solutions, $\alpha_1 = 0$, and another solution α_2 (notice that the degeneracy, $\alpha_2 = \alpha_1 = 0$, occurs only if $\mathbf{f} = \mathbf{f}^{eq}$). In this case, the parameter α^* of the auxiliary population is taken as $\alpha^* = \alpha_2$. This situation can be interpreted as the "bulk case" since both vectors, $\mathbf{f}$ and $\mathbf{f}^*$, are located in the interior of the phase space of populations. The second ("boundary") case corresponds to the situation when Eq. (12) has only one (non-degenerate) solution $\alpha_1 = 0$. Then,

$$\alpha^* = \min_{i=1,\ldots,b;\, \Delta_i < 0} \{ f_i / |\Delta_i| \} \tag{13}$$

The auxiliary state $\mathbf{f}^*$ is taken at the boundary of the phase space (at least one of the populations f_i^* is equal to zero).

The auxiliary population sets the limit of the collision update in such a way that the entropy function H decreases in the result. Once the auxiliary population $\mathbf{f}^*$ is defined, the result of the collision is set as $\mathbf{f}(\beta) = (1-\beta)\,\mathbf{f} + \beta \mathbf{f}^*$ where β is a fixed parameter chosen on the segment $[0, 1]$. Convexity of the entropy function implies the following inequality (*the local H-theorem*): $H(\mathbf{f}(\beta)) \leqslant H(\mathbf{f})$. Moreover, when approaching the hydrodynamic regime, i.e., close enough to the local equilibrium, only the bulk case is realized because $\mathbf{f}^{eq}$ for Boltzmann-like entropy functions is a positive vector. Then the parameter β controls the viscosity coefficient in the resulting Navier–Stokes equations in the following way: The zero viscosity limit corresponds to $\beta \to 1$. Thus, in the ELBM, population vector is updated according to kinetic equation,

$$\mathbf{f}(x + \mathbf{c},\, t+1) - \mathbf{f}(x,\, t) = \mathbf{\Delta}^*[\mathbf{f}(x,\, t)] \tag{14}$$

where $\mathbf{\Delta}^*$ is *dressed* (or *stabilized*) collision integral,

$$\mathbf{\Delta}^*[\mathbf{f}(x,\, t)] = \beta \alpha[\mathbf{f}(x,\, t)]\, \Delta[\mathbf{f}(x,\, t)] \tag{15}$$

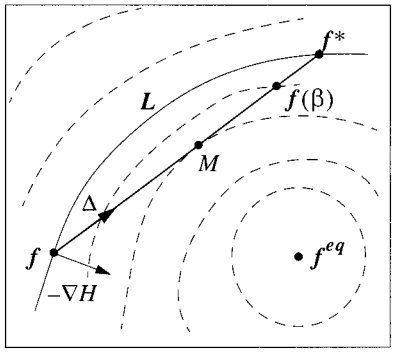

Fig. 1. Stabilization procedure. Curves represent entropy levels, surrounding the local equilibrium $\mathbf{f}^{eq}$. The solid curve L is the entropy level with the value $H(\mathbf{f}) = H(\mathbf{f}^*)$, where $\mathbf{f}$ is the initial, and $\mathbf{f}^*$ is the auxiliary population. The vector Δ represents the collision integral, the sharp angle between Δ and the vector $-\nabla H$ reflects the entropy production inequality. The point $\mathbf{M}$ is the solution to the Eq. (32). The result of the collision update is represented by the point $\mathbf{f}(\beta)$. The choice of β shown corresponds to the "overrelaxation": $H(\mathbf{f}(\beta)) > H(\mathbf{M})$ but $H(\mathbf{f}(\beta)) < H(\mathbf{f})$. The particular case of the BGK collision (not shown) would be represented by a vector Δ_{BGK}, pointing from $\mathbf{f}$ towards $\mathbf{f}^{eq}$, in which case $\mathbf{M} = \mathbf{f}^{eq}$.

In other words, bare collision integrals are stripped off any relaxation time parameters, and are merely directions in the space of populations, pointing towards the change of the state in the collision event. Parameter α defines the maximal admissible collision step along this direction so that the entropy will not decrease. The combination $(\beta\alpha)^{-1}$ is the effective relaxation time in the fully discrete kinetic picture. A graphical interpretation is provided in Fig. 1.

5. DERIVATION OF THE VISCOSITY

Identification of the viscosity coefficient in the ELBM is done on the basis of the Chapman–Enskog analysis[12] in the vicinity of the local equilibrium, in the same way as in the standard Lattice Boltzmann realizations. We will specify the exact form of the collision integral in the next section, but for now we assume that it is a member of the family of admissible collision integrals.

Linearization of the dressed collision integral (15) may be written as,

$$\delta\Delta^* = \beta\alpha(\mathbf{f}^{eq})\,\mathbf{L}\delta\mathbf{f} \tag{16}$$

Here $\mathbf{L}$ is the linearized bare collision integral, and $\alpha_{eq} = \alpha(\mathbf{f}_{eq})$ is found upon expanding equation (12) at equilibrium to the first nontrivial

(quadratic) order. [Note that a substitution of $\mathbf{f}^{eq}$ into Eq. (12) does not give an equation for α_{eq}. This is natural because, by its sense, α_{eq} is a relaxation parameter which can be only specified by considering deviations from the equilibrium.] The result reads:

$$\alpha_{eq} = -\frac{2\langle \delta\mathbf{f} | \nabla\nabla H(\mathbf{f}^{eq}) | \mathbf{L}\delta\mathbf{f} \rangle}{\langle \mathbf{L}\delta\mathbf{f} | \nabla\nabla H(\mathbf{f}^{eq}) | \mathbf{L}\delta\mathbf{f} \rangle} \tag{17}$$

Here $\nabla\nabla H(\mathbf{f}^{eq})$ is the $b \times b$ matrix of second derivatives of the entropy function at equilibrium. Equation (17) suggests that, in general, α_{eq} has a spectrum of values dependent on the direction along which the equilibrium is approached. However, drastic simplification of Eq. (17) happens if $\mathbf{L}$ has the projector property:

$$\mathbf{LL} = -\mathbf{L} \tag{18}$$

In this case, relaxation parameter α_{eq} becomes independent of the direction in the phase space, along which the state relaxes to the equilibrium. This is the essence of the SRTM which simply tells that all the $b-n$ kinetic variable relax to zero with the same rate. This important property is satisfied, in particular, by the linearized bare BGK collision integral, and it has been already demonstrated elsewhere[10] that in this case $\alpha_{eq} = 2$. Thus, Eq. (16) together with Eq. (18) defines the linearized dressed collision integral,

$$\delta\mathbf{\Delta}^* = 2\beta\mathbf{L}^*\delta\mathbf{f} \tag{19}$$

where, operator $\mathbf{L}^*$ has the projector property given by Eq. (18). With this description of the linearized dressed collision integral, we now follow the standard Chapman–Enskog analysis, and seek the solution to the kinetic equation (14) in the form, $\mathbf{f} = \mathbf{f}^{eq} + \delta\mathbf{f}^{ne}$, where the nonequilibrium part $\delta\mathbf{f}^{ne}$ is orthogonal to the hydrodynamic subspace, $\langle \{\mathbf{1}, \mathbf{c}_\alpha\} \mid \delta\mathbf{f}^{ne} \rangle = \{0, 0\}$, and is found in terms of the expansion, $\delta\mathbf{f}^{ne} = \epsilon\delta\mathbf{f}^{(1)} + \epsilon^2\delta\mathbf{f}^{(2)} + O(\epsilon^3)$, subject to the multiscale expansion of the time and space derivatives, $\partial_t = \epsilon\partial_t^{(1)} + \epsilon^2\partial_t^{(2)} + O(\epsilon^3)$, $\partial_\alpha = \epsilon\partial_\alpha^{(1)} + O(\epsilon^2)$. Then,

$$-2\beta \sum_j L_{ij}^* \delta f_j^{(1)} = [\partial_t^{(1)} + c_{i\alpha}\partial_\alpha] f_i^{eq} \tag{20}$$

$$-2\beta \sum_j L_{ij}^* \delta f_j^{(2)} = \partial_t^{(2)} f_i^{eq} + [\partial_t^{(1)} + c_{i\alpha}\partial_\alpha] \left[-\beta \sum_j L_{ij}^* \delta f_j^{(1)} + \delta f_i^{(1)} \right] \tag{21}$$

By the Fredholm alternative, solution to Eq. (20) is written as,

$$\delta \mathbf{f}^{(1)} = \delta \mathbf{f}^{(1)}_{\text{spec}} + \delta \mathbf{f}^{(1)}_{\text{hom}} \tag{22}$$

where $\delta \mathbf{f}^{(1)}_{\text{hom}}$ is the general solution to the homogeneous equation, $\mathbf{L}^* \delta \mathbf{f}^{(1)}_{\text{hom}} = 0$, and $\delta \mathbf{f}^{(1)}_{\text{spec}}$ is a special solution to the inhomogeneous equation (20). The homogeneous solution is equal to zero by the orthogonality condition mentioned above.

Using the projector property (18), Eqs. (20) and (21) are equivalent to the following two equations for the special solution (we omit the subscript spec):

$$-2\beta \delta f_i^{(1)} = [\partial_t^{(1)} + c_{i\alpha}\partial_\alpha]\, f_i^{\text{eq}} \tag{23}$$

$$-2\beta \delta f_i^{(2)} = \partial_t^{(2)} f_i^{\text{eq}} + (1-\beta)[\partial_t^{(1)} + c_{i\alpha}\partial_\alpha]\, \delta f_i^{(1)} \tag{24}$$

The latter set of equations coincides with the well known case of the LBGK, in which the BGK relaxation parameter τ^{-1} is replaced by 2β, and we are immediately led to the following viscosity coefficient

$$\nu = \frac{c_s^2(1-\beta)}{2\beta} \tag{25}$$

Thus, the ELBM is able to retain the full control over the viscosity, while variation of the parameter β in the interval $[0, 1]$ covers the full linear stability interval.

Finally, it should be stressed that the theoretical derivation of the viscosity coefficient is always strictly applicable only in the vicinity of the local equilibrium.

6. THE SINGLE RELAXATION TIME MODEL FOR THE COLLISION INTEGRAL

It is important to notice that simplification of the near-equilibrium dynamics with the projector property [Eq. (18)] concerns solely the linearized bare collision integral, but does not tell yet anything about situations far from equilibrium. There might be many collision integrals which have the same property [Eq. (18)] near equilibrium but different elsewhere. Our goal is therefore to construct a nonlinear SRTM which has the desired projector property [Eq. (18)] near equilibrium (and thus is equivalent to

the linearized BGK), and requires only the knowledge of the entropy function.

In order to construct the SRTM, we first write operator $\mathbf{L}$ with the property (18) in terms of a given basis of the kinetic subspace $\mathbf{g}_s$:

$$\mathbf{L} = -\sum_{s=1}^{b-n} |\mathbf{g}_s\rangle\langle\mathbf{g}_s| \tag{26}$$

We seek the SRTM within the following family of admissible collision integrals:

$$|\Delta\rangle = -\sum_{s,\,p=1}^{b-n} |\mathbf{g}_s\rangle\, K_{sp}(\mathbf{f})\langle\mathbf{g}_p\,|\,\nabla H\rangle \tag{27}$$

Here K_{sp} are elements of a positive definite $(b-n)\times(b-n)$ matrix $\mathbf{K}$. Functions K_{sp} may depend on the population vector, and any representative of the family (27) is admissible. A requirement that the linearization of the collision integral (27) equals $\mathbf{L}$ (26) uniquely defines matrix $\mathbf{K}$ at equilibrium:

$$\begin{aligned} \mathbf{K}(\mathbf{f}^{\mathrm{eq}}) &= \mathbf{C}^{-1}(\mathbf{f}^{\mathrm{eq}}) \\ C_{sp}(\mathbf{f}^{\mathrm{eq}}) &= \langle\mathbf{g}_s|\,\nabla\nabla H(\mathbf{f}^{\mathrm{eq}})\,|\mathbf{g}_p\rangle \end{aligned} \tag{28}$$

Finally, we need to extend the the matrix $\mathbf{K}(\mathbf{f}^{\mathrm{eq}})$ to arbitrary $\mathbf{f}$. This extension is not unique but we suggest the most simple approach which amounts to replacing $\mathbf{f}^{\mathrm{eq}}$ by $\mathbf{f}$ in the Eq. (28) to give

$$\begin{aligned} \mathbf{K}(\mathbf{f}) &= \mathbf{C}^{-1}(\mathbf{f}) \\ C_{sp}(\mathbf{f}) &= \langle\mathbf{g}_s|\,\nabla\nabla H(\mathbf{f})\,|\mathbf{g}_p\rangle \end{aligned} \tag{29}$$

Matrix $\mathbf{C}(\mathbf{f})$ is symmetric and positive definite for any $\mathbf{f}$ (the last statement follows from the strict convexity of the entropy function for any $\mathbf{f}$). Then $\mathbf{C}^{-1}$ exists for any $\mathbf{f}$, and it it is straightforward to prove that the resulting matrix $\mathbf{K}(\mathbf{f})$ is positive definite for any $\mathbf{f}$. In this case we find the nonlinear SRTM given by Eqs. (27) and (29). Notice that the matrix $\mathbf{K}(\mathbf{f})$, and all the other elements in Eq. (27), are well defined once only the entropy function is known.

As far as the choice of the set of basis vectors is concerned, any orthonormal set of basis vectors which lie in the null space of conservation vectors will suffice. However, one would like to have a set of basis vector which will make matrix C as sparse as possible. Our suggestion for basis vector is,

$$
\begin{aligned}
g_1 &= \frac{1}{\sqrt{6}}(-2,\ 0,\ 0,\ 0,\ 0,\ 1,\ 0,\ 1,\ 0)^T \\
g_2 &= \frac{1}{2}(0,\ 1,\ -1,\ 1,\ -1,\ 0,\ 0,\ 0,\ 0)^T \\
g_3 &= \frac{1}{\sqrt{30}}(2,\ 0,\ 0,\ 0,\ 0,\ 2,\ -3,\ 2,\ -3)^T \\
g_4 &= \frac{1}{\sqrt{12}}(0,\ -2,\ 0,\ 2,\ 0,\ 1,\ -1,\ -1,\ 1)^T \\
g_5 &= \frac{1}{\sqrt{12}}(0,\ 0,\ -2,\ 0,\ 2,\ 1,\ 1,\ -1,\ -1)^T \\
g_6 &= \frac{1}{\sqrt{180}}(4,\ -5,\ -5,\ -5,\ -5,\ 4,\ 4,\ 4,\ 4)^T
\end{aligned}
\tag{30}
$$

where, the conservation vectors are,

$$
\begin{aligned}
e_\rho &= \frac{1}{3}(1,\ 1,\ 1,\ 1,\ 1,\ 1,\ 1,\ 1,\ 1)^T \\
e_{v_x} &= \frac{1}{\sqrt{6}}(0,\ 1,\ 0,\ -1,\ 0,\ 1,\ -1,\ -1,\ 1)^T \\
e_{v_y} &= \frac{1}{\sqrt{6}}(0,\ 0,\ 1,\ 0,\ -1,\ 1,\ 1,\ -1,\ -1)^T
\end{aligned}
\tag{31}
$$

Using this choice of basis vector matrix C can be inverted analytically.

7. IMPLEMENTATION OF THE ENTROPY ESTIMATE

The next important point concerns solving the nonlinear equation (12), which implements the discrete time H-theorem. Because the entire ELBM is largely based on convexity of the entropy function, and also because working with Boltzmann-like H-functions cannot tolerate any nonpositivity of populations, it is desirable to avoid conventional methods which do not respect positivity and convexity. Our approach to solve Eq. (12) is based on a two-side estimate of the location of the nontrivial root. The upper bound $\alpha_{\max} > 0$ is the minimal solution to the equations, $f_i + \alpha \Delta_i = 0$, $\Delta_i < 0$. In geometrical terms, $\alpha_{\max}$ corresponds to the point on the boundary of the kinetic polytope where the ray, $\mathbf{f}(\alpha) = \mathbf{f} + \alpha \mathbf{\Delta}$, $\alpha \geqslant 0$,

intersects the boundary. Construction of the lower bound, $\alpha_{\min}$, is based on the earlier general study of the initial layer problem in dissipative kinetics.[13, 14] Specifically, we consider another nonlinear equation,

$$\langle \nabla H(\mathbf{f}+\alpha\Delta) \mid \Delta \rangle = 0 \tag{32}$$

In geometrical terms, the unique solution to this equation, $\alpha_{\min}$, defines population vector $\mathbf{f}_{\min} = \mathbf{f} + \alpha_{\min}\Delta$ which is the minimum entropy state on the ray $\mathbf{f}(\alpha)$. Indeed, the minimum condition is the tangency point of the ray to a level of entropy function (see Fig. 1). The nontrivial solution to Eq. (12) is strictly in the interval $[\alpha_{\min}, \alpha_{\max}]$. In order to evaluate $\alpha_{\min}$, we have applied a quasi-Newton method of ref. 13 which guarantees successive approximations, $\alpha_{\min}^{(n)}$, $n = 1,\ldots$, and for all n it is valid that $0 < \alpha_{\min}^{(n)} \leqslant \alpha_{\min}$. Moreover, the first approximation, $\alpha_{\min}^{(1)}$ is known analytically [see ref. 13]. This estimate of lower bound is given as,

$$\alpha_{\min}^{(1)} = \frac{1-\exp(-\sigma/q)}{\mu+\nu\exp(-\sigma/q)} \tag{33}$$

with,

$$\text{the entropy production} \qquad \sigma = -\langle \nabla H \mid \Delta \rangle \tag{34}$$

$$\text{the maximum loss in the population} \qquad \mu = \max(\Delta_i^- / f_i) \tag{35}$$

$$\text{the total gain in the population} \qquad \nu = \frac{1}{q}\sum \frac{(\Delta_i^+)^2}{f_i} \tag{36}$$

$$\text{and the normalization factor} \qquad q = \sum \Delta_i^+ \tag{37}$$

where, the collision integral Δ is partitioned in positive (Δ^+) and negative ($-\Delta^-$) parts such that,

$$\Delta_j^+ = \begin{cases} \Delta_j & \text{if} \quad \Delta_j > 0 \\ 0 & \text{else} \end{cases} \tag{38}$$

and,

$$\Delta_j^- = \begin{cases} -\Delta_j & \text{if} \quad \Delta_j < 0 \\ 0 & \text{else} \end{cases} \tag{39}$$

This estimate for $\alpha_{\min}^{(1)}$ guarantees that the solution is located strictly inside the interval $[\alpha_{\min}^{(1)}, \alpha_{\max}]$. Starting with this bound for the root, the bisection method has been implemented. The present algorithm of solving for the

entropy condition [Eq. (12)] guarantees that positivity of populations is not violated.

The method of implementation for the entropy estimate described above is quite general. The method can be implemented for any entropy function. However, in the present case we know that α should be very close to 2. Using this information, we have refined the root solver by using a combination of the Newton–Raphson method and of the bisection method, which usually converges to the root in less than 10 iteration. This minimizes computational overhead for solving the nonlinear equation.

In general, the ELBM has to perform two extra steps in comparison to the LBGK scheme. The first step is computation of the bare collision integral, Eq. (29). The second step is to solve the nonlinear equation (12). Both of these operations scale linearly with the number of lattice nodes.

At each time step, the root solving will require $b \times N \times X$ evaluation of the function $f_i \log(C_i f_i)$. The collision integral in Eq. (29) require N times evaluation and inversion of a symmetric positive definite matrix of dimension $(b-M)\times(b-M)$. This is of the order $O(N(b-M)^3/6+(b-M)(b-M+1)/2)$ operation. Here X is the number of iteration required to solve Eq. (12), and M is the number of the conservation laws. Notice that the collision matrix in the standard LBGK is diagonal and any improvement over LBGK has to deal at least with the evaluation of the collision matrix of the size $(b-M)\times(b-M)$. One such example is the recently proposed method[15] based on the linear stability analysis. To give a reader a concrete feel of the numbers involved, on a Sun workstation for a grid size of 21×21 doing 10000 time steps simulation with the present scheme took around 130 seconds while with the BGK time involved was around 13 seconds. A BGK simulation of 10000 time steps for a grid size of 63×63 took around 120 seconds. Thus, the present scheme is an order of magnitude slower compared to the BGK. In the present scheme around 80% of the time is spent for evaluating the collision operator. On the other hand, time required to solve for the entropy estimates contributes only around 5–10% to the total computation time. In the present work, we have focused on the optimization of the entropy estimate, optimization of the collision operator is left for the future work.

8. SOME NUMERICAL RESULTS

8.1. Shock Tube Tests

The first example presented here is from ref. 5, the time evolution of a one-dimensional front in a shock tube, a very classical problem in which it appears a compressive shock front moving in the low density and a

rare-faction front moving in the high density region. These two fronts leave an intermediate region in the central portion of the tube with uniform density ρ_c, and uniform velocity u_c. The tube is filled at time $t=0$ with a gas at rest with uniform density $\rho_-(u_-=0)$ for $x<0$, and $\rho_+(u_+=0)$ for $x>0$. For the inviscid case, $\nu=0$, the density and the velocity profiles present a discontinuity across the shock.

Simulations were performed in order to compare the stability of the three LBM algorithms: The nonlinear LBM[16] (LBE hereafter), the LBGK method with the polynomial equilibrium ansatz,[3] and the present ELBM algorithm.

At $t=0$ the lattice was populated as to give the density $\rho_-=1.5$ for $0\leqslant x\leqslant 400$, and $\rho_+=0.75$ for $400<x\leqslant 800$. Standard bounce back boundary conditions were applied at both ends of the tube. Results for the three algorithms are demonstrated in Figs. 2 and 3 for a relatively high value of viscosity $\nu=3.3333\times 10^{-2}$. It has been found that the LBGK and the ELBM never showed divergence even when the viscosity was smaller than $\nu<10^{-3}$. However, in contrast to the ELBM, the results of the LBGK demonstrate large fluctuations already at $\nu<1$. For this reason, results of the ELBM were always better in comparison to the LBGK at low viscosity.

8.2. Two-Dimensional Simulations

To compare the present algorithm with the standard LBGK method, we have chosen the setup of the two-dimensional Poiseuille flow. Stability of both the schemes has been investigated with respect to various perturbations. In the first set of experiments, non-hydrodynamic perturbations were used, keeping mean velocity at each node intact. In particular, populations at the different nodes were perturbed by a small amount in a way similar to that proposed in ref. 17 for fluctuating hydrodynamics. However, noise is switched on only at a fixed time t_0, typically after the velocity profile has been developed up to its steady state (parabolic) shape.

In another set of numerical experiments, the fully developed velocity profile has been perturbed by adding a small amount of velocity u_y at each node, at time t_0, in a way consistent with the boundary conditions. We have tried two different perturbations, one which respect divergence freedom of the incompressible fluid and the other one which do not respect this condition. In particular, the following perturbations have been used (the origin of the coordinate system is at the central node at the inlet, the reduced x coordinate, $-1\leqslant x\leqslant 1$ is taken across the channel):

$$\begin{aligned}\delta(\rho u_y) &= 0.005 u_{y\max}\sin(\omega\pi y)\\ \delta(\rho u_x) &= 0\end{aligned} \tag{40}$$

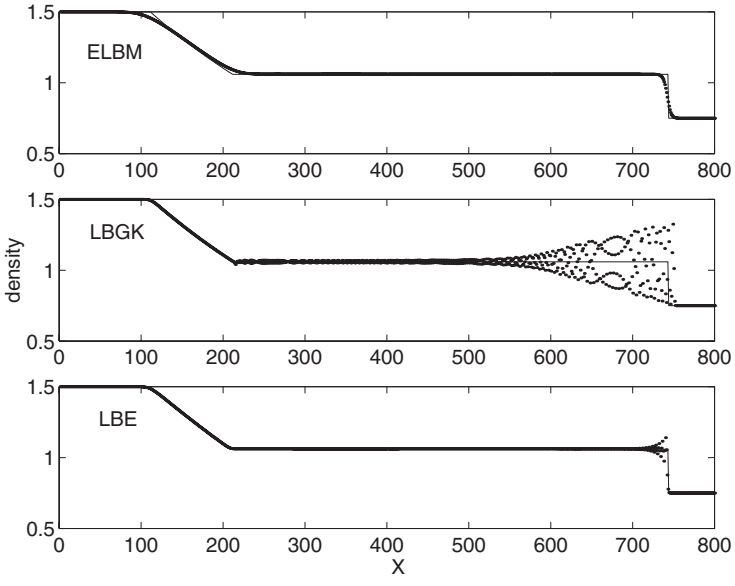

Fig. 2. Density profile for a One-dimensional shock tube simulation (dimensionless lattice units) at $t = 500$ for viscosity $\nu = 3.3333 \times 10^{-2}$. Thin line: Exact solution. Symbol: Simulation.

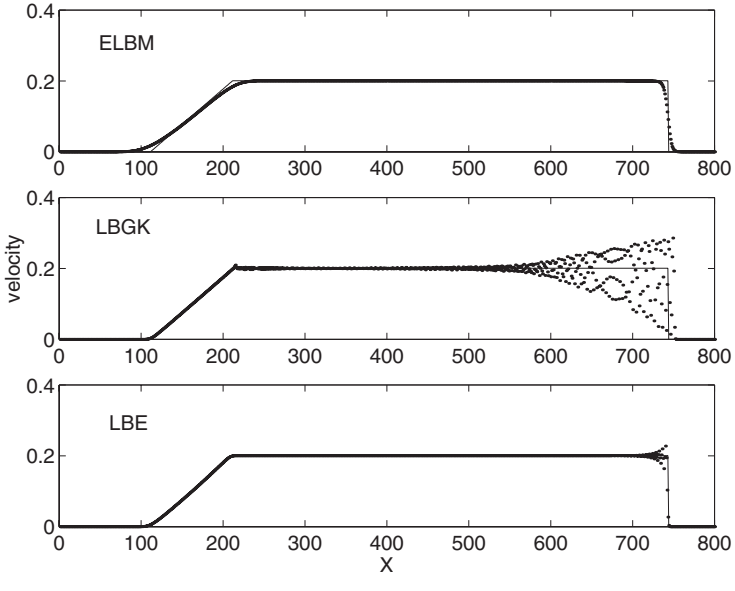

Fig. 3. Velocity profile. Simulation setup and notation same as in Fig. 2.

and,

$$\begin{aligned}\delta(\rho u_y) &= 0.005 u_{y\max} \sin(\omega\pi y)\\ \delta(\rho u_x) &= -0.005\omega\pi x u_{y\max} \cos(\omega\pi y)\end{aligned} \tag{41}$$

for all the nodes except for the bounce-back nodes. On the nodes where the bounce-back has been applied, the perturbation has been set equal to zero, $\delta(\rho u_y) = \delta(\rho u_x) = 0$. The first perturbation [Eq. (40)] does not respect the divergence freedom of the incompressible fluid, while the second perturbation [Eq. (41)] respect the divergence condition. In all experiments, the excess total kinetic energy, $\Delta E(t) = \sum_{\mathbf{r}} [u^2(\mathbf{r}, t_0 + t) - u^2(\mathbf{r}, t_0)]$, has been monitored for $t \geqslant t_0$. The present scheme demonstrates a rapid decay of the excess kinetic energy (as it should be), whereas $|\Delta E|$ grows in the LBGK scheme [see Figs. 4–6].

The present algorithm is unconditionally stable, and for arbitrary low values of the viscosity never runs into the overflow, while the minimal value of the viscosity at which the standard LBGK algorithm converges back to the correct fully developed velocity profile is of the order of $\nu_{\min}^{\mathrm{LBGK}} \sim 10^{-3}$. We have also tested the stability of the LBGK against the

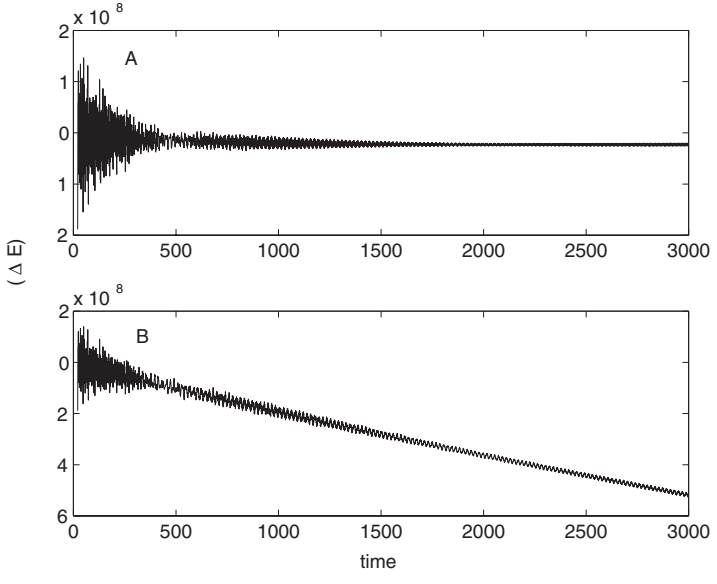

Fig. 4. Time behavior of the excess kinetic energy ΔE after a random perturbation in the population. (A) ELBM, $\nu = 8.3752 \times 10^{-4}$ ($\beta = 0.995$), $u_{y\max} = 1.8059 \times 10^{-3}$. (B) LBGK, $\nu = 8.3752 \times 10^{-4}$ ($\beta = 0.995$), $u_{y\max} = 1.805925 \times 10^{-3}$. The curve terminates after an overflow at $t \approx 10^5$.

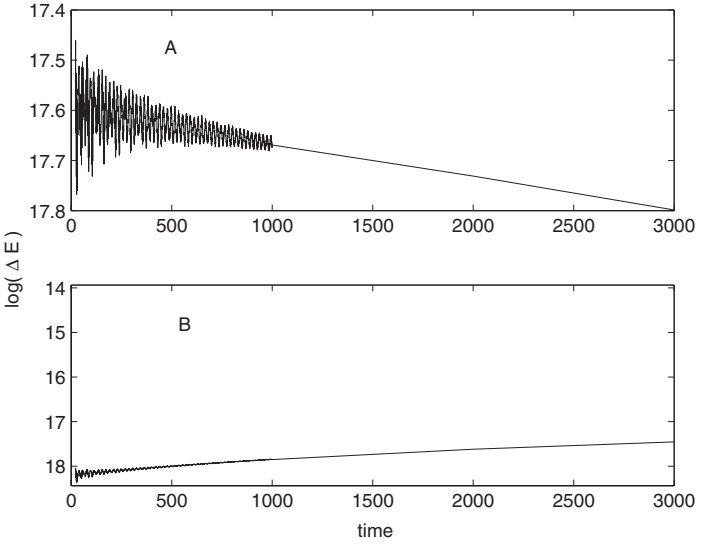

Fig. 5. Time behavior of the excess kinetic energy ΔE after the velocity perturbation (40) with $\omega = 3$. (A) ELBM, $\nu = 8.3752 \times 10^{-4}$ $(\beta = 0.995)$, $u_{y\,\max} = 1.8059 \times 10^{-3}$. (B) LBGK, $\nu = 1.6836 \times 10^{-3}$ $(\beta = 0.99)$, $u_{y\,\max} = 1.3476 \times 10^{-3}$. The curve terminates after an overflow at $t \approx 10^6$.

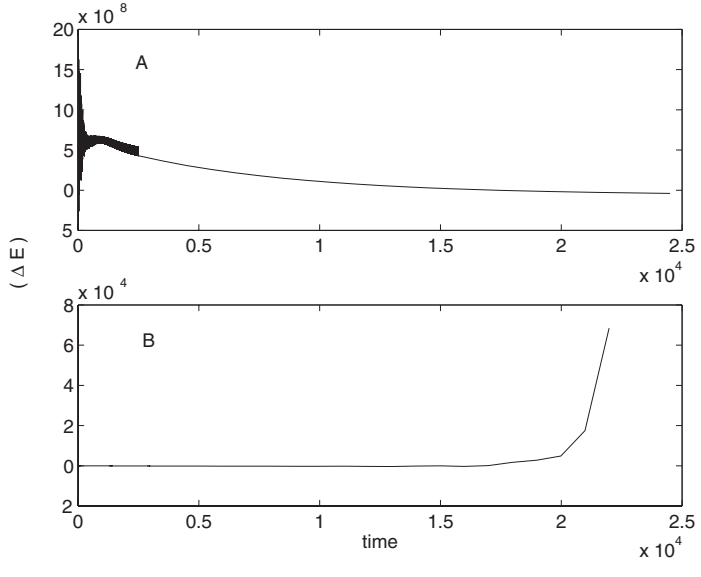

Fig. 6. Time behavior of the excess kinetic energy ΔE after the velocity perturbation (41) with $\omega = 3$. (A) ELBM, $\nu = 1.683502 \times 10^{-3}$ $(\beta = 0.99)$, $u_{y_{\max}} = 5.39055 \times 10^{-3}$. (B) LBGK, $\nu = 1.683502 \times 10^{-3}$ $(\beta = 0.99)$, $u_{y_{\max}} = 5.39055 \times 10^{-3}$.

random perturbation by doubling the number of nodes in each direction. The stability of the LBGK has not improve by this increase in the system size.

9. CONCLUSION

We have demonstrated how the Lattice Boltzmann method can be equipped with the H-theorem to enhance its stability. We have shown that for realization of LBM an explicit knowledge of equilibrium distribution is not necessary, only the knowledge entropy function is sufficient to construct the algorithm. Further development of the Lattice Boltzmann modeling can be based on the construction of the entropy function specific to the physical problem under consideration.

A few concluding remarks to compare the present work with the work of Boghosian *et al.*[9] are in order. First, the main goal of their work was to give a general description of the kinetic polytopes, whereas our focus is on the implementation of the ELBM for a specific choice of the entropy function which recovers the Navier–Stokes equation. Second, in the work[9] solving numerically for the equilibrium distribution function at each time step is proposed, while in the present work a new collision operator is proposed which circumvents the need for solving a set of non-linear equations at each time step to get the equilibrium distribution function. Finally we have introduced a solver for the entropy estimate which guarantees positivity of the populations.

ACKNOWLEDGMENTS

We acknowledge stimulating discussions with L. S. Luo, H. C. Öttinger, S. Succi, and A. J. Wagner.

REFERENCES

1. Excellent reviews of the Lattice Boltzmann method can be found in:S. Chen and G. D. Doolen, *Annu. Rev. Fluid Mech.* **30**:329 (1998); R. Benzi, S. Succi and M. Vergassola, *Phys. Rep.* **222**:147 (1992); A. J. C. Ladd, *J. Fluid Mech.* **271**:285 (1994); Y. H. Qian, J. Lebowitz, and S. Orszag, eds., Special issue on Lattice Gas, *J. Stat. Phys.* **81** (1995); Y. H. Qian, S. Succi and S. Orszag, *Ann. Rev. Comp. Phys.* **3**:195 (1995).
2. H. Chen, S. Chen, and W. H. Matthaeus, *Phys. Rev. A* **45**:R5339 (1992).
3. Y. H. Qian, D. d'Humiéres, and P. Lallemand, *Europhys. Lett.* **17**:479 (1992).
4. I. V. Karlin, A. Ferrante, and H. C. Öttinger, *Europhys. Lett.* **47**:182 (1999).
5. S. Ansumali and I. V. Karlin, *Phys. Rev. E* **47**:7999 (2000).
6. F. J. Higuera, S. Succi, and R. Benzi, *Europhys. Lett.* **9**:345 (1989).
7. F. Toschi, G. Amati, S. Succi, R. Benzi, and R. Piva, *Phys. Rev. Lett.* **82**:5044 (1999).

8. S. Ansumali and I. V. Karlin, manuscript (2000).
9. B. M. Boghosian, J. Yepez, P. V. Coveney, and A. Wagner, *Proc. Roy. Soc. Lond A MAT* **457**:717 (2001).
10. I. V. Karlin, A. N. Gorban, S. Succi, and V. Boffi, *Phys. Rev. Lett.* **81**:6 (1998).
11. A. J. Wagner, *Europhys. Lett.* **44**:144 (1998).
12. S. Chapman and T. Cowling, *The Mathematical Theory of Non-Uniform Gases* (Cambridge University Press, Cambridge, 1970).
13. Constructive estimations of the state **M** for a generic kinetic equation are given in A. N. Gorban, I. V. Karlin, V. B. Zmievskii, and T. Nonnenmacher, *Physica A* **231**:648 (1996).
14. A. N. Gorban, I. V. Karlin, and V. B. Zmievskii, *Transport Theory Stat. Phys.* **28**:271 (1999).
15. P. Lallemand and L.-S. Luo, *Phys. Rev. E* **61**:6546 (2000).
16. Y. H. Qian, D. d'Humières, and P. Lallemand, *Adv. in Kinetic Theory and Continuum Mechanics*, R. Gatignol and Soubbaramayer, eds. (Springer, Berlin, 1991), p. 127.
17. A. J. C. Ladd, *J. Fluid Mech.* **271**:285 (1994).